

Structure and magnetism of Co(II) complexes with bidentate heterocyclic ligand *Hsalbim* derived from benzimidazole

M. Šebová^a, V. Jorík^b, J. Moncol^b, J. Kožíšek^c, R. Boča^{a,b,*}

^a Department of Chemistry, FPV, University of SS Cyril and Methodius, Trnava, Slovakia

^b Institute of Inorganic Chemistry, Technology and Materials, FCHPT, Slovak University of Technology, SK-812 37 Bratislava, Slovakia

^c Institute of Physical Chemistry, FCHPT, Slovak University of Technology, 812 37 Bratislava, Slovakia

ARTICLE INFO

Article history:

Received 16 September 2010

Accepted 17 January 2011

Available online 3 February 2011

Keywords:

Co(II) complexes

Magnetism

Heterocyclic ligands

Zero-field splitting

ABSTRACT

Two mononuclear Co(II) complexes based upon 2-(1*H*-benzimidazol-2-yl)phenol, abbreviation *Hsalbim* ligand, have been prepared and studied. The structure of *Hsalbim* and [Co(*salbim*)₂] have been confirmed by X-ray structure analysis. The second cobalt(II) complex matches the formula [Co(*salbim*)₂](*Hsalbim*)-MeOH assuming a co-crystallization of one neutral ligand. The electronic spectra are consistent with the tetrahedral pattern. Magnetic susceptibility measurements down to *T* = 2 K along with the magnetization data until *B* = 7 T show that the Co(II) complexes are high-spin with a considerable zero-field splitting of the ⁴B₁(D_{2d}) term: *D*/*h**c* = 67 and 55 cm⁻¹, respectively.

© 2011 Elsevier Ltd. All rights reserved.

1. Introduction

Heterocyclic N-donor ligands are widely used in assembling complexes which exhibit interesting magnetic properties. For instance, the spin crossover systems, high-spin molecules and molecular ferromagnets represent new materials that are promising in technical exploitation [1,2]. Herein we focused to three heterocyclic ligands that contain benzimidazole unit linked to the other ring containing donor (N or O) atoms (Fig. 1). The Co(II) complexes of *salbim*, in comparison with available data for analogous *poxbim* and *pybzim* ligands, represent the center of interest of the present communication.

The compound 2-(1*H*-benzimidazol-2-yl)phenol, abbreviated as *Hsalbim*, was first prepared by reacting salicylamide with 1,2-diaminobenzene [3]. It has been used in analytical chemistry as selective agent in determining mercury. It can be prepared by condensation of salicylic acid with 1,2-diaminobenzene in presence of P₂O₅, or using a catalyst SiCl₄, and *p*-toluenesulfonic acid [4].

We will focus to the cobalt(II) complexes formed of the ligand LH = *Hsalbim*; only two tetra-coordinate complexes, [Co^{II}L₂] and [Co^{II}L₂]-DMF, were structurally characterized so far [5,6] whereas *mer*-[Co^{III}L₃]-3EtOH·H₂O is a hexacoordinate complex [7].

The compound LH = *Hsalbim* (CCDC name HAVBIQ [8]) for the polymorph-1 and HAVBIQ01 [7] for the polymorph-2, can exist in various tautomeric forms (protonated and deprotonated) as

shown in Fig. 2. Therefore it could act as a versatile ligand whose properties are tunable by changing pH of the reaction mixture. Numerous complexes of this ligand exist as documented by entries in the CCDC database. The ligand LH preferentially coordinates as a bidentate-anionic unit, L⁻, forming tetra-coordinate complexes (Sol means a co-crystallized solvent): [Co^{II}L₂] – KATHAP [5], [Co^{II}L₂]-Sol – RODWEN [6], [Zn^{II}L₂] – HAVBOW [8], [Zn^{II}L₂]-Sol – GEPDAH [9], KANYEE [10] and UFONAF [11], [Cu^{II}L₂] – XIHNIM [12], [Cu^{II}L₂]-Sol – MAVKAW [13], and [Be^{II}L₂] – QAQFIY [14]. Hexacoordination occurs in [Fe^{III}L₂(O₂N)]-Sol – TOQQOG [15] and [Cr^{III}L₂phen]⁺-Sol – FURSOB [16]. The tris-L⁻ coordination is exemplified by [Co^{III}L₃]-Sol – OGAMUF [7]. Interesting compound is a hexacoordinate complex [Mn^{III}(LH)(py)(MeOH)]-MeOH – DEFREM [17], where both, the neutral and the anionic forms of the ligand coexist. A bridging ability of the L⁻ ligand is exemplified by [ClCu^{II}L₂]-Sol – TEWJIP [18]. However, in the binuclear complex [(HO)Fe^{III}L₂]₂-Sol – TOQQUM the L⁻ unit acts as a terminal ligand [15]. A rather surprising is a monodentate O-coordination of the ligand L⁻ in [Sn^{IV}LPh₃EtOH] – VOPCUZ [19] and its analogs [19] VOPDAG, VOPDEK and VOPDIO as opposed to [Sn^{IV}L₂Ph₂]-Sol – VOPDOU and VOPDOU01. A rare example of the unioordination exists in *trans*-[Re^VLCl₂OPPh₃] – IGEWUN [20], *cis*-[Re^VLCl₂OPPh₃] – IGEXAU [20], and their analogs [20] IGEXEY, IGEXIC and IGEXOI. On the contrary, bis-L⁻ coordination occurs in [Re^VL₂O(OMe)]-Sol – IGEXUO [20].

The condensation product of pyridinecarboxaldehyde *N*-oxide with 1,2-diaminobenzene yields a ligand 2-(2-benzimidazolyl)-pyridine *N*-oxide, hereafter *poxbim*, which has been isolated in a free form and structurally characterized – XELDIB [21]. The bidentate ligand gave a series of complexes with Mn(II), Fe(II), Co(II),

* Corresponding author. Tel.: +421 259325610.

E-mail address: roman.bocha@stuba.sk (R. Boča).

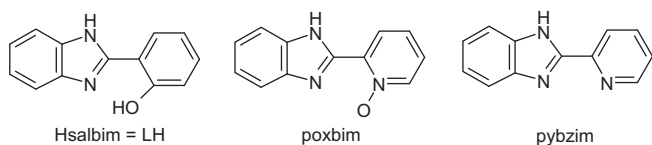


Fig. 1. Heterocyclic compounds used as ligands.

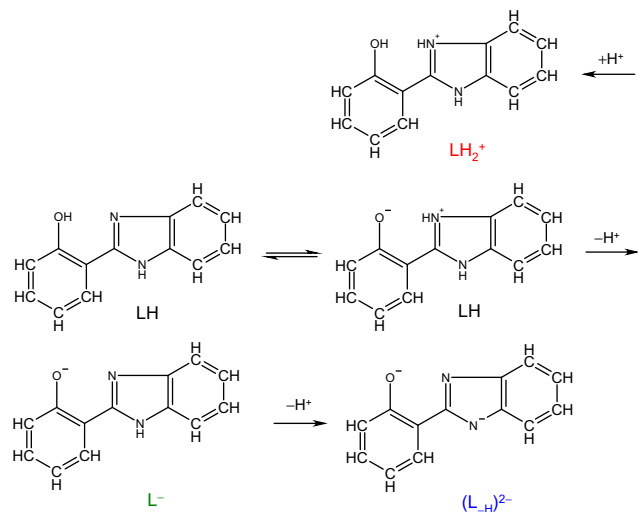


Fig. 2. Various forms of the ligand LH = Hsalbim.

Ni(II), Cu(II) and Zn(II) with 1:1, 1:2, 1:3, 1:4 and 1:5 metal-to-ligand ratios. The hexacoordination has been confirmed by X-ray structure for $[\text{Co}^{\text{II}}(\text{poxbim})_2(\text{H}_2\text{O})_2](\text{ClO}_4)_2$ – XELDOH [21]. Unusual molar ratio M:L = 1:4 has been rationalized by X-ray structure of $[\text{Zn}(\text{poxbim})_2(\text{H}_2\text{O})_2](\text{ClO}_4)_2 \cdot (\text{poxbim})_2$ where two ligands coordinate, but two neutral solvent molecules lie outside the coordination sphere – XELDUN [21]. The central unit possesses the *trans*- $\{\text{MOw}_2\text{N}_2\text{O}_2\}$ chromophore.

The family of complexes with the neutral *pybzim* ligand, 2,2'-(benzimidazol-2-yl)pyridine, is richer. However, only three complexes with Co(II) have been structurally characterized so far and they possess a polymeric structure: JEXNOQ [22], TINRUE [23], and WEXQUM [24]. With the deprotonated ligand only two mononuclear complexes of Co(III) were reported: $[\text{Co}(\text{pybzim})_3] \cdot 2(\text{acetone}) \cdot 1.33\text{H}_2\text{O}$ – OGAMOZ [7] and $[\text{Co}(\text{pybzim})_3] \cdot 2\text{DMF} \cdot \text{H}_2\text{O}$ – KOKFUL [25].

2. Experimental

2.1. Synthesis

The compound **1**, *Hsalbim* = 2-(1H-benzimidazol-2-yl)phenol, was prepared from 12.7 g (0.092 mol) of salicylic acid and 10.0 g (0.092 mol) freshly recrystallized 1,2-diaminobenzene in 100 cm³ (1.48 mol) of phosphoric acid (80%). The reaction mixture was heated and stirred for 24 h at temperature of 160–180 °C. After cooling, dark-blue reaction mixture was dissolved in 1000 cm³ of distilled water to form dark blue solution. The suspension was saturated by Na₂CO₃ until neutral pH and extracted in 400 cm³ of hot methanol. Insoluble solid fraction was and then separated by filtration. The filtrate, after cooling, gave a crude crystalline product that was isolated by filtration. The final product of lilac color was obtained by recrystallization from methanol. Yield 4.2 g (22%). *Anal.* Calc. for C₁₃H₁₀N₂O (*M* = 210.24): C, 74.3; H, 4.79; N, 13.3. Found: C, 74.3; H, 4.78; N, 13.3%.

The compound **2**, $[\text{Co}^{\text{II}}(\text{salbim})_2]$, has been prepared as follows. A solution of 0.18 g (0.49 mmol) of $\text{Co}(\text{ClO}_4)_2 \cdot 6\text{H}_2\text{O}$ in 5 cm³ of water and 7 cm³ of hot methanol was slowly added to the solution of 0.21 g (0.49 mmol) of *Hsalbim* in 35 cm³ of hot methanol under an intense stirring. The dark-pink solution was boiled for 30 min. The mixture was cooled to r.t. under stirring and then the dark-pink product was separated. The product was dissolved in 50 cm³ of acetone, filtered, washed with small amount of water and ethanol and then dried on air. Yield 0.10 g (47%). *Anal.* Calc. for C₂₆H₁₈N₄O₂Co (*M* = 477.39): C, 65.4; H, 3.80; N, 11.7. Found: C, 64.3; H, 3.88; N, 11.3%.

The compound **3** was prepared from 0.08 g (0.21 mmol) $\text{Co}(\text{ClO}_4)_2 \cdot 6\text{H}_2\text{O}$ dissolved in 10 cm³ of water. The solution was stirred under heating, and warm solution of 0.1 g (0.47 mmol) of *Hsalbim* dissolved in 10 cm³ of MeOH was added. The rose color solution was stirred under heating for 30 min. The product was isolated by filtration and left to dry on air. Yield 0.08 g (53%). The isolated material in form of pearl-pink flakes does not allow the X-ray structure determination. *Anal.* Calc. for C₄₀H₃₂N₆O₄Co (*M* = 719.67, **3** = 2·*Hsalbim*·MeOH): C, 66.8; H, 4.48; N, 11.7. Found: C, 66.5; H, 4.75; N, 11.2%.

The infrared spectra for **2** and **3** contain the basic features given by the free ligand **1** (Supplementary material, Fig. S1). The spectra for **2** and **3** are remarkably similar with some additional features in **3** due to the solvent molecules. An additional, rather sharp peak at 1026 cm⁻¹ is assigned to the C–O stretching vibration most probably from the MeOH which was used in synthesis. Formulation of the complex **3** in the form of a solvated **2**, **3** = 2·Sol, is consistent with available structural data. The presence of a free ligand in the complex **3** is confirmed by the TG/DTA analysis: the mass loss until 150 °C is 3.4% (liberation of the methanol) and then proceeds very gradually (with only a slight endothermic effect) until 400 °C where $\Delta m = 17.5\%$ (liberation of uncoordinated *Hsalbim* molecules). Then the mass loss is more abrupt until the end of the heating (500 °C) where it is accompanied with a strong exothermic effect (decomposition of the complex $[\text{Co}(\text{salbim})_2]$) – see Supplementary material, Fig. S2.

2.2. Physical measurements

Elemental analysis was carried out on FlashEA 1112 (Thermo-Finnigan). IR spectra were measured in KBr pellets (Magna FTIR 750, Nicolet) in the 400–4000 cm⁻¹ region. Electron spectra were measured in Nujol mull (Specord 200, Analytical Jena) in the range 9000–50000 cm⁻¹. TG/DTA analysis has been done with Shimadzu apparatus (DTG60).

The powder diffraction patterns have been measured with X-ray powder diffractometer (Philips) using Co-anode ($\lambda = 1.78892 \text{ \AA}$).

Magnetic data were taken with the SQUID magnetometer (MPMS-XL7, Quantum Design) using the RSO mode of detection. The susceptibility data were scanned in the temperature range 2–300 K at the applied field of *B* = 0.1 T. The magnetization has been measured at *T* = 2.0 and 4.6 K. Raw data were corrected for the underlying diamagnetism using estimate of χ_{dia} ($10^{-12} \text{ m}^3 \text{ mol}^{-1}$) = –5 M [g mol⁻¹].

2.3. X-ray crystallography

Data collection and cell refinement of **1** and **2** were carried out using a κ -axis diffractometer Gemini R CCD (Oxford Diffraction) with graphite monochromated Mo K α radiation. The diffraction intensities were corrected for Lorentz and polarization factors. The structures were solved by direct methods using SIR-97 [26] or SHELXS-97 [27] and refined by the full-matrix least-squares procedure with SHELXL-97 [27]. The analytical absorption correction

Table 1
Crystallographic data for **1** and **2**.

Compound	1	2
Chemical formula	C ₁₃ H ₁₀ N ₂ O	C ₂₆ H ₁₈ CoN ₄ O ₂
<i>M</i>	210.23	477.37
Cell setting, space group	orthorhombic, <i>Pna</i> 2 ₁	monoclinic, <i>P</i> 2 ₁ / <i>c</i>
<i>T</i> (K)	293(2)	293(2)
<i>a</i> (Å)	18.2406(5)	10.1590(10)
<i>b</i> (Å)	4.7989(2)	10.0280(9)
<i>c</i> (Å)	11.9979(3)	21.450(2)
β (°)	90	94.597(9)
<i>V</i> (Å ³)	1050.23(6)	2178.2(4)
<i>Z</i>	4	4
Radiation type	Mo K α	Mo K α
μ (mm ⁻¹)	0.087	0.820
Crystal size (mm)	0.626 × 0.536 × 0.099	0.191 × 0.186 × 0.082
Diffractometer	Gemini R CCD	Gemini R CCD
Absorption correction	analytical	analytical
<i>T</i> _{min} , <i>T</i> _{max}	0.954, 0.992	0.727, 0.864
<i>S</i>	1.050	1.008
<i>R</i> ₁ [<i>F</i> ₂ > 2 σ (<i>F</i> ₂)], <i>wR</i> ₂ (<i>F</i> ₂)	0.0284, 0.0749	0.0734, 0.157
Data/restraints/parameters	2127/1/146	4437/0/308
$\Delta\rho_{\max}$, $\Delta\rho_{\min}$ (e Å ⁻³)	0.098, -0.136	0.479, -0.349
CCDC code	793545	793546

[28] was made by using CRYSLIS-RED [29]. Geometrical analyses were performed with SHELXL-97. The structures were drawn with MERCURY [30] and/or XP in SHELXTL [27]. Crystal data, conditions of data collection, and refinement information are reported in Table 1.

3. Results and discussion

3.1. Structural data

The compound *Hsalbim* (**1**) gave suitable single crystals from methanol. It is a planar molecule where N1–C1 [1.359(2) Å], and N2–C1 [1.322(2) Å] bond lengths indicate that the whole molecule is conjugate (Fig. S3, Supplementary material). The crystal structure of **1** shows two types of intermolecular hydrogen bonds which

create *R*₂¹(7) rings [31] and yield a supramolecular chain (Fig. 3B). A hydrogen bond between (*iz*)NH and the hydroxyl oxygen atom N1–H1A···O1 [2.00 Å], as well as much weaker intermolecular interaction C9–H9A···O1 [2.81 Å] are registered. A stronger intramolecular hydrogen bond exists between the (O)H···N(*iz*): O1–H1···N2 [2.550(1) Å].

Similar structure of **1** (HAVBIQ, orthorhombic) has been reported for *Hsalbim* recrystallized from chloroform [8]. However, a monoclinic polymorph (HAVBIQ01) has been isolated by recrystallization of *Hsalbim* from DMSO [7]. The crystal structure of the monoclinic form of *Hsalbim* also shows two types of intermolecular hydrogen bonds (Fig. 3A) that result in a supramolecular chain; the intermolecular interaction C10–H10A···N2 is weaker and the hydrogen bonds create *R*₃²(8) rings [31].

The complex **2** crystallizes in the monoclinic system and the centrosymmetric space group *P*2₁/*n*, but molecules of [Co(*salbim*)₂] do not occupy special positions (Fig. 4). On the other hand, the tetragonal polymorph of [Co(*salbim*)₂] – KATHAP [5], which is a racemic twin (space group *P*4₁2₁2), contains the Co atom at the twofold axis. In **2** the two bidentate *salbim*-*N,O* ligands form a distorted tetrahedral chromophore {CoN₂O₂}; the angle between the Co1/N1/O1 and Co1/N3/O2 planes is 89° (Fig. S4). The bond lengths Co1–O1 (1.909(3) Å), Co1–O2 (1.913(3) Å), Co1–N1 (1.976(4) Å) and Co1–N3 (1.958(4) Å) in **2** are similar to those found in the tetragonal form of [Co(*salbim*)₂] (KATHAP) [5] and also in the complex [Co(*salbim*)₂]:2DMF (RODWEN) [6]. Analogous geometry of the chromophore exists in other {Co^{II}N₂O₂} complexes with derivatives of *salbim* as ligands: GAJTER [32], GAJTIV [32], GAJTOB [32], and WIPMAJ [33].

Hydrogen bonds in the crystal structure of monoclinic and tetragonal forms of [Co(*salbim*)₂] are drawn in Fig. 5. The complex molecules of **2** are linked by intermolecular hydrogen bonds between (*iz*)NH and phenolate oxygen atoms of adjacent complex molecules in **2**: N2–H2N···O2ⁱ and N4–H4N···O1ⁱⁱ [symmetry codes: (i) $-x + 3/2, y + 1/2, -z + 3/2$; (ii) $-x + 1, -y, -z + 1$] with N···O separations of 2.811(5) and 2.830(5) Å, respectively; a two-dimensional hydrogen-bonding network is formed (Fig. S5). Two molecules in **2** are linked to *R*₂²(12) ring [31] through

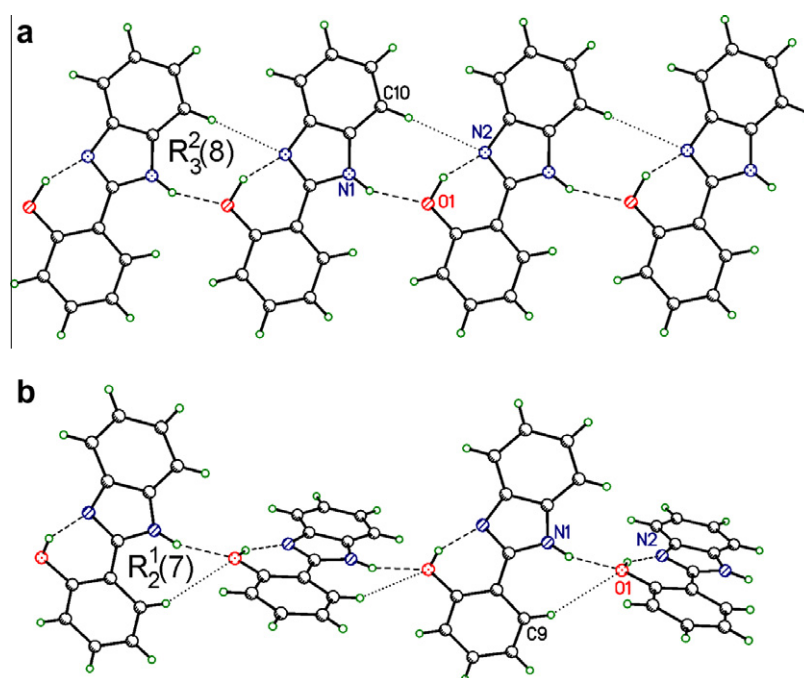


Fig. 3. Different hydrogen bond networks in two polymorphs of *Hsalbim*: (a) monoclinic HAVBIQ01 [7], (b) this work, similar to orthorhombic HAVBIQ [8].

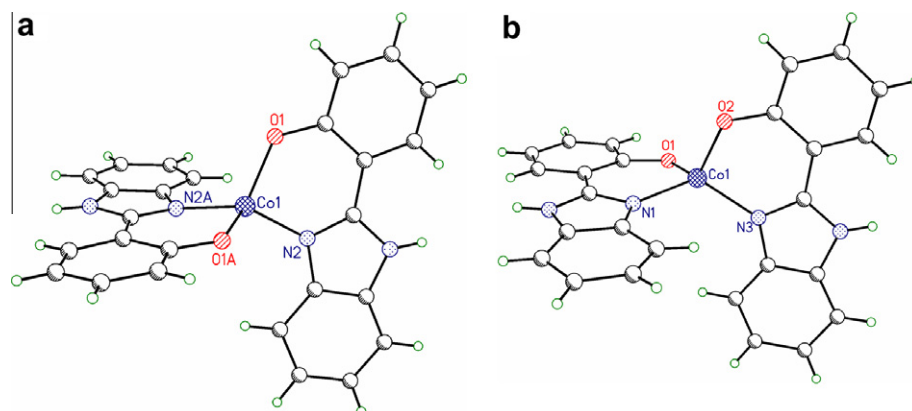


Fig. 4. The molecular structure of two polymorphs of $[\text{Co}(\text{salbin})_2]$: (a) one part of a racemic twin of KATHAP in space group $P4_12_12$ [5], (b) complex **2** in $P2_1/n$.

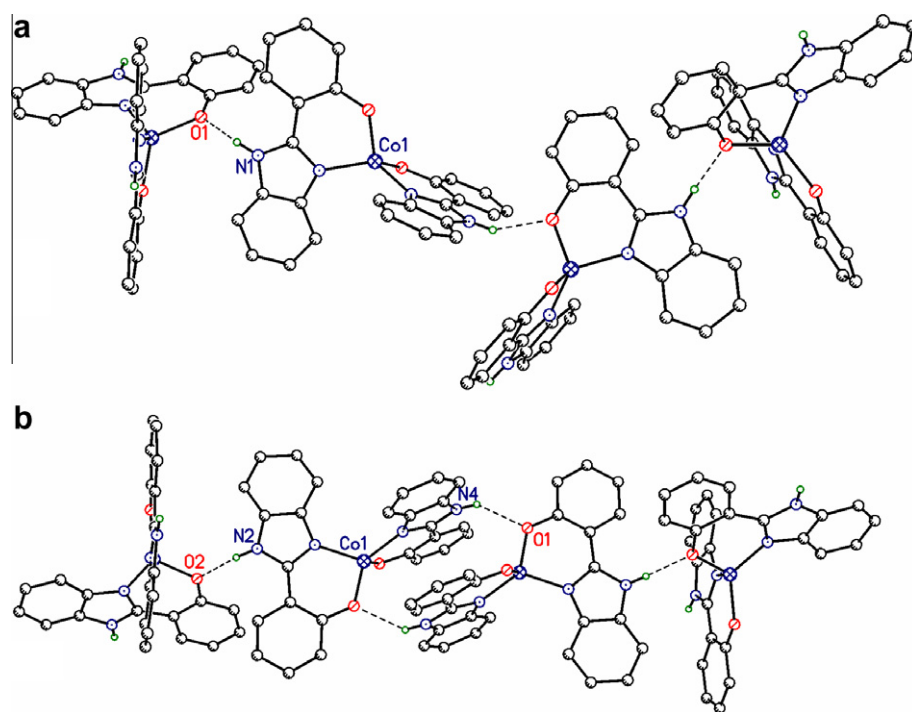


Fig. 5. The molecules of $[\text{Co}(\text{salbin})_2]$ connected through N–H...O bonds: (a) in KATHAP; (b) in the complex **2**.

$\text{N4}–\text{H4N} \cdots \text{O1}^{\text{ii}}$ hydrogen bonds. There are π – π stacking interactions [34] between and the [C13–C19] benzene rings of *salbin* ligands and adjacent symmetry-related [C21–C26] benzene ring of *salbin* ligands at $(x + 1/2, -y + 1/2, +z + 1/2)$; centroid...centroid distance is 3.73 Å and distances between two benzene planes are in the range 3.30–3.80 Å. On the other hand, crystal structure of KATHAP [5] exhibits a three-dimensional hydrogen-bonding network (Fig. S6). It can be concluded that **2** and KATHAP represent supramolecular isomers [35–37] with different hydrogen-bonding networks.

3.2. Powder diffraction patterns

In general, the cobalt complexes display a variety of instabilities and interconversions. First, the Co(II) complexes are sometimes oxidized to Co(III) and the Co(III) ones are kinetically inert. Second, Co(II) complexes are susceptible for isomerism among which the salt isomerism is quite common. Even if the X-ray structure had been done, there is no guarantee that the powder material was

identical with that piece of the single crystal. Therefore the powder diffraction technique is a powerful tool in proving the identity and purity of the powder material.

The powder diffraction patterns have been taken for compounds **1** through **3**. The patterns have been reconstructed from the available X-ray structure data by MERCURY [30].

According to Fig. 6 the powder of LH = *Hsalbin* is identical with the crystalline polymorph-2 (HAVBIQ01). This differs from the XPD of the polymorph-1 (HAVBIQ) that matches the present X-ray structure redetermination (**1**).

The X-ray structure for **2** has been solved in the space group $P4_12_12$ as a racemic twin (KATHAP [5]). In this case all unit cell angles were 90°. The theoretical powder diffraction pattern is presented in Fig. 7. The present structure redetermination refers to the space group $P2_1/n$ where the angle $\beta = 94.597(9)^\circ$ in the monoclinic crystal system. This manifests itself in a different powder diffraction pattern where the first line is markedly split. The recorded XPD pattern for **2** matches a theoretical prediction based upon the full structural determination.

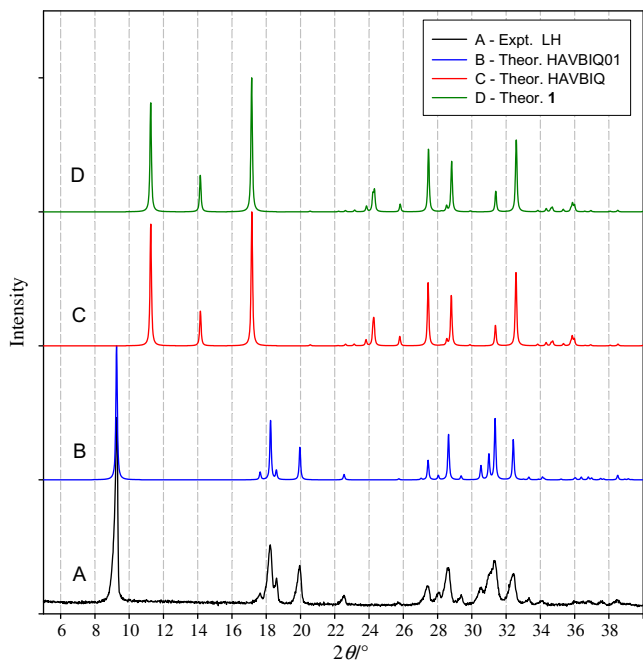


Fig. 6. Powder diffraction patterns for the free ligand *Hsalbim*.

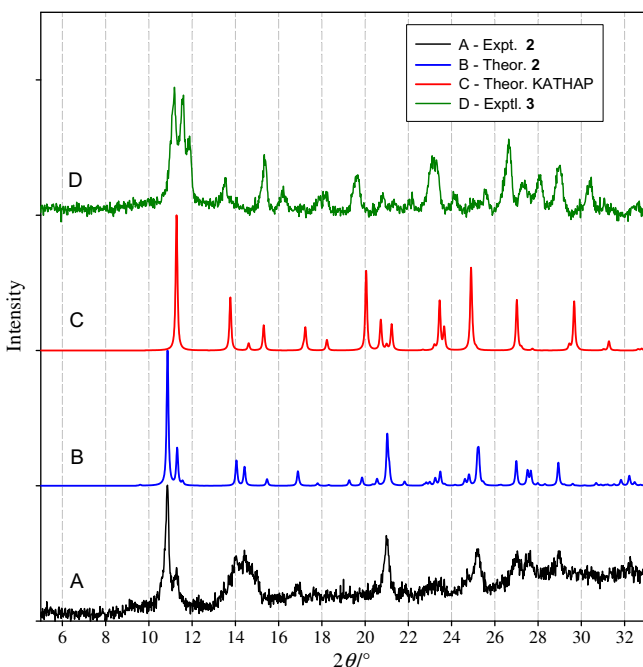


Fig. 7. Powder diffraction patterns for the Co(II) complexes of *salbim*.

The XPD data for **3** unambiguously shows that this sample is different from **2**. However, any embodiment of the solvent molecules will change the lattice parameters and consequently the whole XPD pattern. Therefore it cannot be excluded that the compound **3** is **2**-Sol. This hypothesis is supported by inspecting the CCDC-database according to which the M^{II} centers form with the *salbim* ligand exclusively $[M^{II}L_2]$ -Sol complexes.

3.3. Electronic spectra

The electronic spectrum of **2** (Fig. 8) in the range of 9000–23 000 cm^{-1} exhibits a number d–d transitions which are followed

by an intense charge transfer band. The d–d transitions are well visible at 10 400 (a broad band), 18 000, and 19 200 (narrow) cm^{-1} ; there is shoulder at 17 000 cm^{-1} . Since the structure of the complex **2** has been determined as tetrahedral, and the powder diffraction pattern matches the theoretical prediction, the interpretation of the spectrum should be done in the T_d group of symmetry in the first approximation.

The estimate for the crystal field strength for tetrahedral systems is $Dq(T_d) = (4/9)Dq(O_h) = (4/9)(1/6)F_4(R)$. Therefore the first transition $\Delta_1 (^4A_2 \rightarrow ^4T_2)$ lies in the NIR region and it has not been detected.

The first observed band refers to the $^4A_2 \rightarrow ^4T_1(F)$ transition and its energy is about $\Delta_2 = 18Dq = 10400 \text{ cm}^{-1}$. However, the configuration interaction between $^4T_1(F) \cdot ^4T_1(P)$ terms is effective and causes a reduction of the above estimate. With $Dq = 578$ the estimate for the last allowed d–d transition $^4A_2 \rightarrow ^4T_1(P)$ is $\Delta_3 = 12Dq + 15B$; using the unreduced Racah parameter of Co(II), $B_0 = 980 \text{ cm}^{-1}$, we get $\Delta_3 = 21800 \text{ cm}^{-1}$. This value need be lowered owing to the nephelauxetic effect: the Racah electron repulsion parameter B is reduced relative to its free-ion value B_0 .

The assignment of the bands in the 17000–22000 cm^{-1} region is intricate since the $^4T_{1g}(P)$ mother term is split into $\{^4A_2, ^4E\}$ daughter terms in the more realistic D_{2d} (or C_{2v}) group of symmetry. Moreover, the close-lying $^2E(G)$ term might borrow the intensity from the spin-allowed transitions. The spin-orbit coupling is also in the play and it further modifies the term scheme.

Fortunately, a modeling of the crystal-field terms (and multiplets), as described in details elsewhere [38], brings answer; using the crystal-field poles $F_4 = 8000 \text{ cm}^{-1}$ and $\beta = B/B_0 = 0.90$ the calculated energy spectrum is: 4A_2 (ground state), $^4T_2 - 5925$, $^4T_1(F) - 10\,120$, $^2E(G) - 17\,370$, $^4T_1(P) - 17\,720$, $^2A_1(G) - 20\,830$, $^2T_1(G) - 20\,890$, and $^2T_2(G) - 22\,420 \text{ cm}^{-1}$. Indeed, the terms $^2E(G)$ and $^4T_1(P)$ are close in energy. To this end, the band registered at 18 000 cm^{-1} is assigned to the last allowed d–d transition $^4A_2 \rightarrow ^4T_1(P)$ whereas the shoulder at 17 000 cm^{-1} is assigned to the spin-forbidden transition $^4A_2 \rightarrow ^4E(G)$.

For **3** the d–d transitions are well visible at 10 000–10 700 (a broad band), 15 500 (narrow), 17 100 (narrow) cm^{-1} and 19 000 cm^{-1} (broad). A modeling with $F_4 = 8000 \text{ cm}^{-1}$ and $\beta = B/B_0 = 0.80$ gave the energy spectrum: 4A_2 (ground term), $^4T_2 - 5925$, $^4T_1(F) - 10\,030$, $^2E(G) - 15\,520$, $^4T_1(P) - 15\,850$, $^2A_1(G) - 19\,180$, $^2T_1(G) - 19\,510$, and $^2T_2(G) - 20\,600 \text{ cm}^{-1}$. Again the spin forbidden transition to $^2E(G)$ is close to the last spin allowed transition to $^4T_1(P)$. Accordingly, the registered d–d transitions are assigned as follows: $\Delta_2(^4A_2 \rightarrow ^4T_1(F)) = 10000 \text{ cm}^{-1}$ and $\Delta_3(^4A_2 \rightarrow ^4T_1(P)) = 17100 \text{ cm}^{-1}$. The feature at 15500 cm^{-1} is the $^4A_2 \rightarrow ^2E(G)$ transition that borrows intensity from the close lying allowed transition Δ_3 .

Definitely, the electronic spectrum of **3** is not consistent with octahedral patterns. For an octahedral high-spin Co(II) complex the spin-allowed d–d transitions are $^4T_{1g}(O_h) \rightarrow ^4T_{2g}$, $^4T_{1g} \rightarrow ^4A_{2g}$, and $^4T_{1g} \rightarrow ^4T_{1g}(P)$. Then the d–d transitions refer to $\Delta_1 = 8Dq$, $\Delta_2 = 18Dq$ and $\Delta_3 = 12Dq + 15B$. Taking $\Delta_1 = 8Dq = 10\,000 \text{ cm}^{-1}$, the second band should lie around $\Delta_2 = 18Dq = 22\,500 \text{ cm}^{-1}$ which contradicts to the observation.

The modeling of the electronic spectra has been improved by considering a realistic geometry of the chromophore with the C_{2v} symmetry: the angle $\alpha(N-Co-N) = 129^\circ$, and $\gamma(O-Co-O) = 114^\circ$. The crystal field poles were $F_4(N) = 8500$, and $F_4(O) = 7000 \text{ cm}^{-1}$. The nephelauxetic ratio was $\beta = 0.9$ for **2** and 0.8 for **3**; orbital reduction factors were $\kappa = 0.9$. Within the C_{2v} group of symmetry the energy levels are split into a set of Kramers doublets whereas the spin-orbit coupling only shifts the energy values. According to Fig. 9 the reconstruction of the energy transitions is fairly good. The shoulder at 17 000 cm^{-1} for **2** does not contain a single transition to $^2E(G)$, that is expected to be

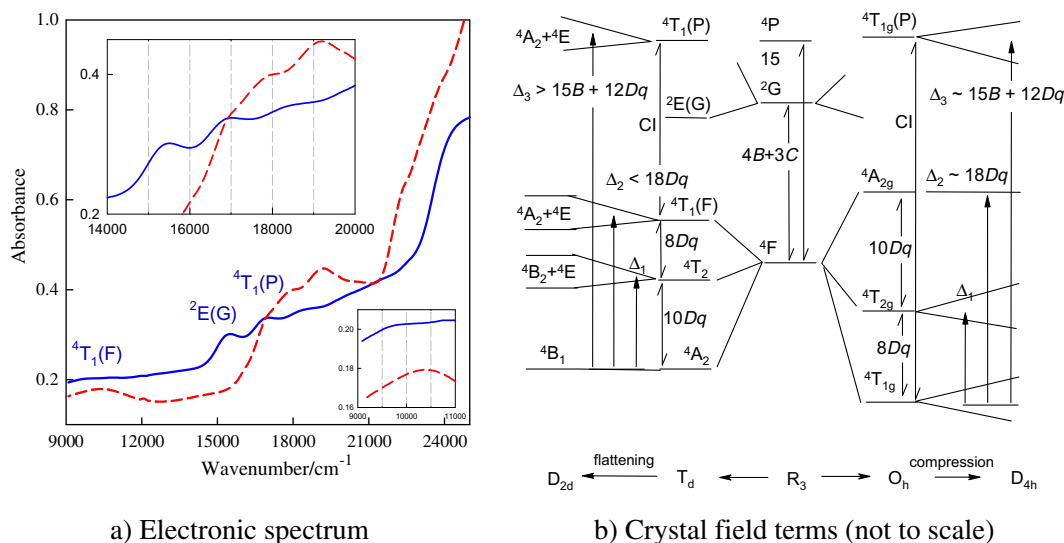


Fig. 8. Electronic spectrum of **2** (dashed) and **3** (solid) measured in Nujol mull.

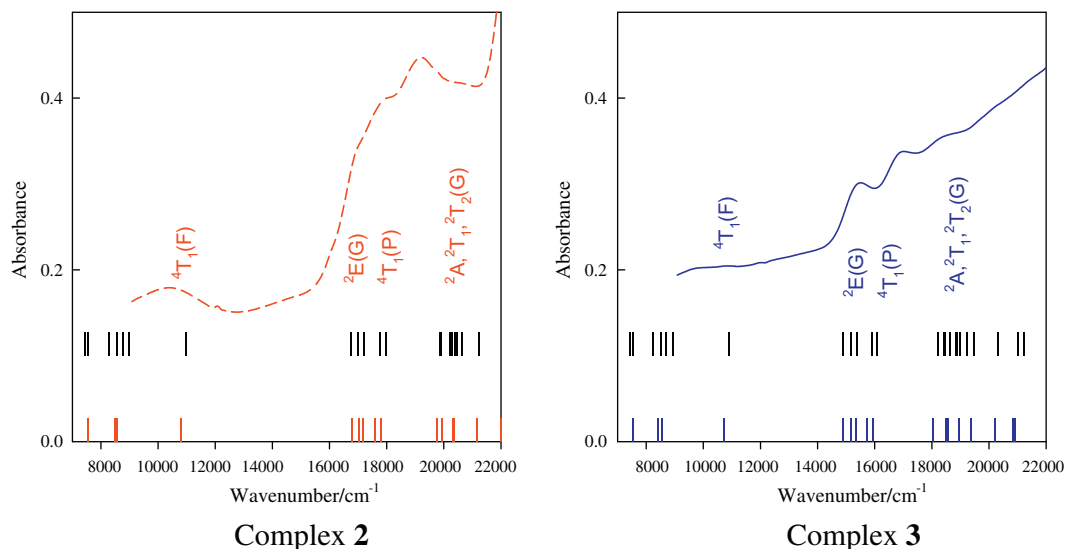


Fig. 9. Modeling of the electronic spectra: horizontal bars – crystal-field terms (lower row) and crystal-field multiplets (upper row).

sharp, but also to a set of transitions to daughter terms of ${}^4T_1(P)$ on symmetry lowering.

The differences in the electronic spectrum for **2** and **3** are probably due to a different degree of flattening of the parent tetrahedra. If this hypothesis is true, then a different zero-field splitting should be detected in magnetic measurements. Notice, the zero-field splitting for a perfect tetrahedron is exactly $D = 0$.

3.4. Magnetic data

The molar magnetic susceptibility for **2**, corrected for the underlying diamagnetism, has been converted to the effective magnetic moment that is displayed in Fig. 10. At the room temperature the value of $\mu_{\text{eff}} = 4.77 \mu_B$ matches the $S = 3/2$ spin system with some orbital contribution to the g -factor ($g \sim 2.5$). On cooling the effective magnetic moment slightly decreases along a straight line which is a fingerprint of some temperature-independent paramagnetism. Below 100 K the decrease is more rapid and reflects the zero-field splitting (the splitting of the ground ${}^4B_1(D_{2d})$ term into two Kramers doublets).

The magnetization data taken at $T = 2.0$ K show a saturation at $B = 7.0$ T but the magnetization per formula unit is only $M_1 = M_{\text{mol}}/(N_A \mu_B) = 2.5$. This subnormal value again reflects a considerable zero-field splitting.

The magnetic data have been fitted by assuming the anisotropic spin Hamiltonian (SH) in the form

$$\hat{H}_a = D[\hat{S}_z^2 - S(S+1)/3]\hbar^{-2} + g_a \mu_B \hat{B}_a \hat{S}_a \hbar^{-1} \quad (1)$$

($a = z, x$) where D is the zero-field splitting parameter and the second contribution is the spin Zeeman term. The anisotropy has been accounted by two different g -factors (g_z and g_x) whereas the D -parameter eventually can be constrained by the SH formula

$$D = \lambda(g_z - g_x)/2 \quad (2)$$

For Co(II) system the value of the spin-orbit splitting parameter is $\lambda = -\zeta_{\text{Co}}/2S$ which amounts to $\lambda/\hbar c = -172 \text{ cm}^{-1}$.

An advanced fitting procedure accounts simultaneously for the two data-sets: $\chi = f(T; B_0 = 0.1 \text{ T})$ and $M = f(B, T_0)$ with $T_0 = 2.0$ and 4.6 K, respectively. The powder average has been done by

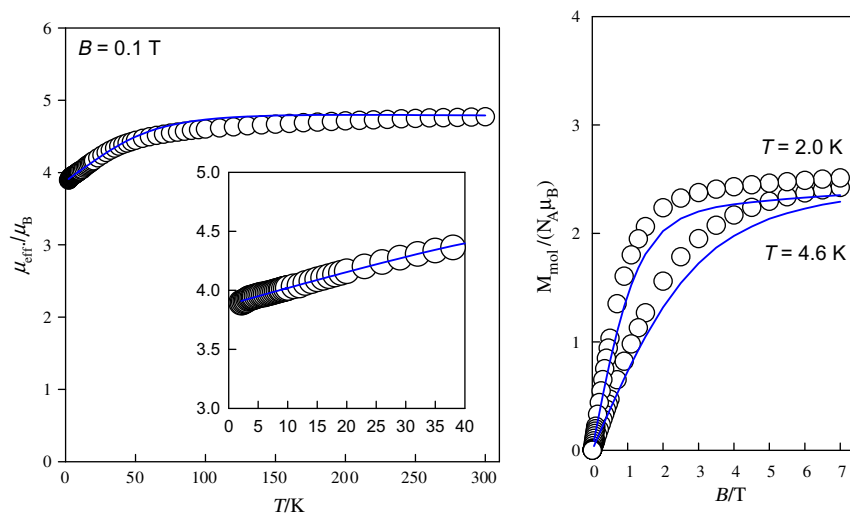


Fig. 10. Magnetic functions for **2** = [Co(*salbim*)₂]. Left – temperature dependence of the effective magnetic moment, right – field dependence of the magnetization. Circles – experimental data. Lines – fitted by $g_z = 2.00$, $g_x = 2.60$, $D/hc = 66.7 \text{ cm}^{-1}$.

averaging 210 points of polar coordinates (ϑ_i, φ_i) distributed over the top hemisphere. It converged to the following set of magnetic parameters: $g_z = 2.00$, $g_x = 2.60$, $D/hc = 66.7 \text{ cm}^{-1}$ [the discrepancy factors $R(\chi) = 0.005$ and $R(M) = 0.098$]. The susceptibility is reproduced excellently, however the magnetization less satisfactory. The involvement of the rhombic zero-field splitting parameter E does not improve the quality of the fit. With the SH formula, the estimate of the axial zero-field splitting parameter is $D/hc = 52 \text{ cm}^{-1}$ that matches the value obtained by optimization.

There is not so much freedom to improve the model unless one considers a multiterm reference. This means a consideration of full space of 120 levels as they result from all terms of the electron configuration d^7 . An alternative is to deal with the spin admixed states – a theory well developed for (quasi) octahedral Fe(III) systems where the spin-orbit coupling operator mixes states of different spin multiplicity $\langle {}^6A_1 | \hat{H}^{so} | {}^4A_1 \rangle$ [38,39]. In the present case the situation is more complex since in addition to $\langle {}^4A_2 | \hat{H}^{so} | {}^2A_2 \rangle$ some other mixings contribute. The principal effect is that in addition to two Kramers doublets arising from the ${}^4A_2(F)$ term another one originating in the ${}^2A_2(G)$ term is in the play, owing to which the overall magnetoactivity is altered (T_d reference group is used for labeling the crystal-field terms).

The experimental magnetic data for **3** are displayed in Fig. 11. It can be seen that the magnetic functions are essentially similar to the complex **2**; the best-fit values for magnetic parameters are $g_z = 2.00$, $g_x = 2.80$, $D/hc = 54.9 \text{ cm}^{-1}$, $\chi_{\text{TIP}} = 26.6 \times 10^{-9} \text{ m}^3 \text{ mol}^{-1}$ [$R(\chi) = 0.009$, $R(M) = 0.048$]. These data again show a considerable magnetic anisotropy represented by the g -factor difference and the zero-field splitting parameter D .

We tested a hypothesis that the complex **3** contains more (less) than one uncoordinated *Hsalbim* molecule. For instance, probing [Co(*salbim*)₂] \cdot 2*salbimH* for **3** would increase the molar mass, giving rise a higher molar magnetization, and consequently to an unrealistically high g -factor.

The zero-field splitting of the order of magnitude $55\text{--}66 \text{ cm}^{-1}$ is high when compared to the other central atoms [40]. However, for hexacoordinate Co(II) complexes D as high as 100 cm^{-1} has been reported [41]. For tetra-coordinate Co(II) complexes $D = 10 \text{ cm}^{-1}$ has been found in $\text{Hg}[\text{Co}(\text{NCS})_4]$, based upon susceptibility measurements [42]. Based upon HF/HF-ESR [43], $D = -14 \text{ cm}^{-1}$ in $[\text{Co}(\text{PPh}_3)_2\text{Cl}_2]$. In Cs_3CoCl_5 the value of $D = -4.3 \text{ cm}^{-1}$ has been detected by HF/HF-ESR whereas in Cs_3CoBr_5 $D = -5.3 \text{ cm}^{-1}$ [44].

The sign of the D -parameter arises from the assignment of the lowest crystal-field multiplet. When the Kramers doublet

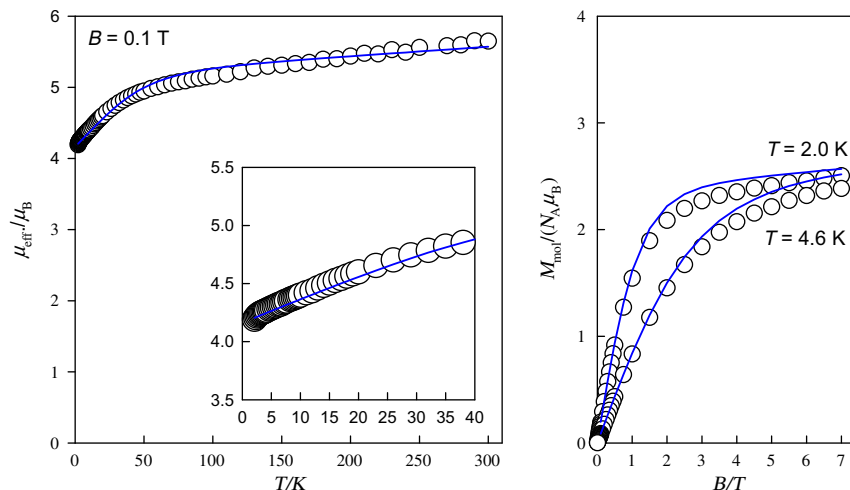


Fig. 11. Magnetic functions for **3** = [Co(*salbim*)₂] \cdot *salbimH* \cdot MeOH. Left – temperature dependence of the effective magnetic moment, right – field dependence of the magnetization. Circles – experimental data. Lines – fitted by $g_z = 2.00$, $g_x = 2.80$, $D/hc = 54.9 \text{ cm}^{-1}$, $\chi_{\text{TIP}} = 26.6 \times 10^{-9} \text{ m}^3 \text{ mol}^{-1}$.

$M_S = \pm 1/2$ is ground state and that $M_S = \pm 3/2$ refers to the excited state, then $\Delta = 2D > 0$ holds true. For instance, the $[\text{CoCl}_4]^{2-}$ ion as found in Cs_3CoCl_5 possesses D_{2d} symmetry and is slightly elongated, while the same anion in Cs_2CoCl_4 has nearly C_{2v} symmetry and is slightly compressed; the former has $D < 0$, and the latter has $D > 0$.

Theoretical modeling with the generalized crystal-field theory gave $D = 10 \text{ cm}^{-1}$ for **2** when the spin-Hamiltonian approximation is used. The splitting of the crystal-field multiplets is $\Delta = 17.8 \text{ cm}^{-1}$ for the orbital reduction factor $\kappa = 0.9$, and 20 cm^{-1} when $\kappa = 1$.

To this end, the present communication represents a step forward in getting magnetostructural D -correlations for Co(II) complexes. These were extensively studied for a series of Ni(II) complexes elsewhere [45–50].

4. Conclusions

The reported X-ray structure data for the complex **2** – $[\text{Co}(\text{salbim})_2]$ is not a simple redetermination of the already published structure (KATHAP) since a different crystal system, different space group and different hydrogen bond network has been found. The measured X-ray powder diffractogram confirms that the powder material used later in magnetic measurements is the complex **2** and not KATHAP. The electronic spectra exhibit transitions that match the tetrahedral pattern. The magnetic data show a considerable zero-field splitting of the $^4B_1(D_{2d})$ ground term ($D/hc = 67 \text{ cm}^{-1}$) which causes a marked deviation of the magnetization from its saturation value as well as a drop of the effective magnetic moment at low temperature.

The composition of the complex **3** = $[\text{Co}(\text{salbim})_2] \cdot \text{salbimH} \cdot \text{MeOH}$ is confirmed by elemental analysis, IR spectra indicating a C–O bond from the methanol solvent, a gradual mass loss on TG/DTA experiments showing first a liberation of MeOH and then liberation of *salbimH*, electron spectra that match a tetrahedral pattern, and magnetic data since $[\text{Co}(\text{salbim})_2]$ will bring too low molar mass and $[\text{Co}(\text{salbim})_2] \cdot 2\text{salbimH}$ too high. The magnetic data again show a considerable zero-field splitting of the $^4B_1(D_{2d})$ ground term ($D/hc = 55 \text{ cm}^{-1}$).

Acknowledgments

Grant agencies (VEGA 1/0213/08, 1/1005/09, APVV 0202-10, VVCE 0004-07) are acknowledged for the financial support.

Appendix A. Supplementary data

CCDC 793545 and 793546 contain the supplementary crystallographic data for **1** and **2**. These data can be obtained free of charge via <http://www.ccdc.cam.ac.uk/conts/retrieving.html>, or from the Cambridge Crystallographic Data Centre, 12 Union Road, Cambridge CB2 1EZ, UK; fax: (+44) 1223-336-033; or e-mail: deposit@ccdc.cam.ac.uk. Supplementary data associated with this article can be found, in the online version, at [doi:10.1016/j.poly.2011.01.021](https://doi.org/10.1016/j.poly.2011.01.021).

References

- [1] O. Kahn, J. Kröber, C. Jay, *Adv. Mater.* 4 (1992) 718.
- [2] D. Gatteschi, *Adv. Mater.* 6 (1994) 635.
- [3] D.A. Horton, G.T. Bourne, M.L. Smythe, *Chem. Rev.* 103 (2003) 893.
- [4] L.J. Walter, H. Freiser, *Anal. Chem.* 25 (1953) 127.

- [5] H.-Y. Bu, Y.-J. Liu, Q.-F. Liu, J.-F. Jia, *Acta Crystallogr.* E61 (2005) m1986 (KATHAP).
- [6] F. He, Y. Xi, J. Li, F. Zhang, *Acta Crystallogr.* E64 (2008) m1311 (RODWEN).
- [7] X. Quezada-Buendia, A. Esparza-Ruiz, A. Pena-Hueso, N. Barba-Behrens, R. Contreras, A. Flores-Parra, S. Bernes, S.E. Castillo-Blum, *Inorg. Chim. Acta* 361 (2008) 2759 (OGAMUF, HAVBIQ01, OGAMOZ).
- [8] Y.-P. Tong, S.-L. Zheng, X.-M. Chen, *Eur. J. Inorg. Chem.* (2005) 3734 (HAVBIQ, HAVBOW).
- [9] Y.-H. Zhao, Z.-M. Su, Y. Wang, X.-R. Hao, K.-Z. Shao, *Acta Crystallogr.* E62 (2006) m2361 (GEPDAH).
- [10] Y.-P. Tong, *Acta Crystallogr.* E61 (2005) m1771 (KANYEE).
- [11] Y.-P. Tong, Y.-W. Lin, *J. Chem. Crystallogr.* 38 (2008) 613 (UFONAF).
- [12] Y.-P. Tong, S.-L. Zheng, *J. Mol. Struct.* 841 (2007) 34 (XIHNM).
- [13] Y. Xi, J. Li, F. Zhang, *Acta Crystallogr.* E61 (2005) m1953 (MAVKAW).
- [14] Y.-P. Tong, S.-L. Zheng, X.-M. Chen, *Inorg. Chem.* 44 (2005) 4270 (QAQFIY).
- [15] A.K. Boudalis, J.M. Clemente-Juan, F. Dahan, V. Psycharis, C.P. Raptopoulou, B. Donnadieu, Y. Sanakis, J.-P. Tuchagues, *Inorg. Chem.* 47 (2008) 11314 (TOQQOQ, TOQQUM).
- [16] Y.-P. Tong, Y.-W. Lin, *Inorg. Chim. Acta* 362 (2009) 2167 (FURSOB).
- [17] W. Shi, Y. Liu, B. Liu, Y. Song, Y. Xu, H. Wang, Y. Sha, G. Xu, S. Styring, P. Huang, *J. Coord. Chem.* 59 (2006) 119 (DEFREM).
- [18] Q.-X. Li, X.-L. Yang, H.-B. Xu, *Chin. J. Struct. Chem.* 26 (2006) 149 (TEWJIP).
- [19] A. Esparza-Ruiz, A. Pena-Hueso, I. Ramos-Garcia, A. Vasquez-Badillo, A. Flores-Parra, R. Contreras, *J. Organomet. Chem.* 694 (2009) 269 (VOPCUZ, VOPDAG).
- [20] B. Machura, M. Wolff, J. Kusz, R. Kruszynski, *Polyhedron* 28 (2009) 2949 (IGEWUN, IGEXAU, IGEXEY, IGEXIC, IGEXOI, IGEXUO).
- [21] M. Vrbová, P. Baran, R. Boča, H. Fuess, I. Svoboda, W. Linert, U. Schubert, P. Wiede, *Polyhedron* 19 (2000) 2195 (XELDOH, XELDUN).
- [22] L.-J. Zhou, Y.-Y.-U. Wang, C.-H. Zhou, C.-J. Wang, Q.-Z. Shi, S.-M. Peng, *Cryst. Growth Des.* 7 (2007) 300 (JEXNOQ).
- [23] C.-K. Xia, W. Wu, Q.-Y. Chen, J.-M. Xie, *Acta Crystallogr.* E63 (2007) m2726 (TINRUE).
- [24] C.-K. Xia, C.-Z. Lu, D.-Q. Yuan, Q.-Z. Zhang, X.-Y. Wu, J.-J. Zhang, D.-M. Wu, *J. Mol. Struct.* 831 (2007) 195 (WEXQUM).
- [25] S.-M. Peng, H.-F. Chen, *Bull. Inst. Chem. Acad. Sin.* 37 (1990) 49 (KOKFUL).
- [26] SIR-97: A. Altomare, M.C. Burla, M. Camalli, G.L. Casciaro, C. Giacovazzo, A. Guagliardi, A.G.G. Moliterni, G. Polidori, R. Spagna, *J. Appl. Crystallogr.* 32 (1999) 115.
- [27] SHELXS-97 and SHELXL-97: G.M. Sheldrick, *Acta Crystallogr.* A64 (2008) 112.
- [28] R.C. Clark, J.S. Reid, *Acta Crystallogr.* A51 (1995) 887.
- [29] Oxford Diffraction, CRYSAIS-CCD and CRYSAIS-RED, Oxford Diffraction Ltd., Abingdon, England, 2010.
- [30] MERCURY: C.F. Macrae, P.R. Edgington, P. McCabe, E. Pidcock, G.P. Shields, R. Taylor, M. Towler, J. van de Streek, *J. Appl. Crystallogr.* 39 (2006) 453.
- [31] J. Bernstein, R.E. Davis, L. Shimoni, N.-L. Chang, *Angew. Chem., Int. Ed. Engl.* 34 (1995) 1555.
- [32] L. Benisvy, E. Bill, A.J. Blake, D. Collison, E.S. Davies, C.D. Garner, C.I. Guindy, E.J.L. McInnes, G. McArdle, J. McMaster, C. Wilson, J. Wolowska, *Dalton Trans.* (2004) 3647 (GAJTOB, GAJTER, GAJTIV).
- [33] J.D. Crane, E. Sinn, B. Tann, *Polyhedron* 18 (1999) 1527 (WIPMAJ).
- [34] C. Janiak, *J. Chem. Soc., Dalton Trans.* (2000) 3885.
- [35] B. Moulton, M.J. Zaworotko, *Chem. Rev.* 101 (2001) 629.
- [36] J.W. Steed, J.L. Atwood, *Supramolecular Chemistry*, second ed., Wiley, Chichester, 2009.
- [37] M. Schröder, N.R. Champness, *Supramolecular isomerism*, in: J.L. Atwood, J.W. Steed (Eds.), *Encyclopedia of Supramolecular Chemistry*, vol. 2, Taylor and Francis, London, 2004, pp. 1420–1423.
- [38] R. Boča, *Struct. Bonding* 117 (2006) 1.
- [39] M. Weissbluth, *Struct. Bonding* 2 (1967) 1.
- [40] R. Boča, *Coord. Chem. Rev.* 248 (2004) 757.
- [41] B. Papánková, R. Boča, Ľ. Dlhán, I. Nemeč, J. Titiš, I. Svoboda, H. Fuess, *Inorg. Chim. Acta* 363 (2010) 147.
- [42] D. Nelson, L.W. ter Haar, *Inorg. Chem.* 32 (1993) 182.
- [43] J. Krzystek, S.A. Zvyagin, A. Ozarowski, A.T. Fiedler, T.C. Brunold, J. Telsler, *J. Am. Chem. Soc.* 126 (2004) 2148.
- [44] R.P. van Staple, H.G. Beljers, P.F. Bongers, H. Zijlstra, *J. Chem. Phys.* 44 (1966) 3719.
- [45] P. Baran, M. Boča, R. Boča, A. Krutošková, J. Miklovič, J. Pelikán, J. Titiš, *Polyhedron* 24 (2005) 1510.
- [46] A. Mašlejová, R. Ivaníková, I. Svoboda, B. Papánková, Ľ. Dlhán, D. Mikloš, H. Fuess, R. Boča, *Polyhedron* 25 (2006) 1823.
- [47] R. Ivaníková, R. Boča, Ľ. Dlhán, H. Fuess, A. Mašlejová, V. Mrázová, I. Svoboda, J. Titiš, *Polyhedron* 25 (2006) 3261.
- [48] J. Titiš, R. Boča, Ľ. Dlhán, T. Durčėková, H. Fuess, R. Ivaníková, V. Mrázová, B. Papánková, I. Svoboda, *Polyhedron* 26 (2007) 1523.
- [49] R. Boča, J. Titiš, In *Coordination Chemistry Research Progress*, Nova Science Publishers, New York, 2008, pp. 247–304.
- [50] J. Titiš, R. Boča, *Inorg. Chem.* 49 (2010) 3971.